2021 International Siberian Conference on Control and Communications (SIBCON) | 978-1-7281-8504-0/20/$31.00 ©2021 IEEE | DOI: 10.1109/SIBCON50419.2021.9438925

Estimation of 4-DoF manipulator optimal configuration for autonomous camera calibration of a mobile robot using on-board templates

Tatyana Tsoy
Laboratory of Intelligent Robotic Systems (LIRS)
Intelligent Robotics Department
Institute of Information Technology and Intelligent Systems
Kazan Federal University
Kazan, Russia

Ramil Safin
Laboratory of Intelligent Robotic Systems (LIRS)
Intelligent Robotics Department
Institute of Information Technology and Intelligent Systems
Kazan Federal University
Kazan, Russia

Evgeni Magid
Laboratory of Intelligent Robotic Systems (LIRS)
Intelligent Robotics Department
Institute of Information Technology and Intelligent Systems
Kazan Federal University
Kazan, Russia

Subir Kumar Saha
Mechanical Engineering Department
Indian Institute of Technology Delhi
New Delhi, India

***Abstract*—Camera calibration is one of the important tasks in the field of robotics and computer vision. It enables to increase the accuracy of metric measurements in photogrammetry applications and provides higher performance in computer vision algorithms such as stereo matching and motion estimation. It is known that regardless of the calibration method used variation of given estimated camera parameters their is inevitable due to multiple reasons: varying weather conditions, temperature fluctuations or severe operation mode of a robotic system. In order to alleviate the aforementioned issues recalibration is required. In this work we employed 4-DoF manipulator Servosila Engineer mobile robotic system equipped with an on-board camera. In order to automate the process of calibration an algorithm is developed which enables to estimate optimal manipulator joint configurations. Forward kinematics is solved on a discretized set of joint angles, subsequently estimating possible camera positions for its further calibration. Experiments on real robot demonstrate the possibility of usage of the developed algorithm to find optimal joint configurations for automatic camera calibration.**

***Index Terms*—camera calibration, manipulator, kinematics, mobile robot**

I. Introduction

Most of computer vision (CV) applications in robotics require a camera installed on a robotic system to be calibrated, e.g. visual simultaneous localization and mapping (SLAM) [1], structure from motion (SfM), teleoperation, path planning, obstacle avoidance [2], visual inspection [3], 3D scene reconstruction, and urban search and rescue (USAR) operations [4]. Camera calibration is the process of estimation of parameters for various camera systems, such as monocular or stereo configurations [5] [6]. Camera parameters establish a mathematical relation between 2D image and 3D world, mapping real objects in the world into pixels in an image plane. Camera calibration helps to increase the accuracy of measurements, i.e. to derive metric information from the images, hence improving performance of CV algorithms.

Z. Zhang distinguishes four groups of camera calibration methods [7]:

- 1D calibration – points on a line undergoing a motion with a fixed point;
- 2D calibration – observing a planar calibration target at different orientations (e.g. checkerboard, circles, and a-circles) [8] [9];
- 3D calibration which makes use of orthogonal planes;
- self-calibration which requires no prior knowledge of camera parameters or objects in the scene [10] [11].

The aforementioned methods that require a particular reference object are referred to as conventional camera calibration approaches. Conversely, self-calibration approaches require neither a calibration objects nor an elaborate system setup [12]. Therefore, it is possible to use self-calibration methods in the main pipeline along with other CV algorithms, e.g. object detection and tracking. Nevertheless, self-calibration methods are prone to errors in a higher degree compared to the conventional approaches [13]. 2D calibration objects, such as a checkerboard pattern or fiducial markers [14] [15], can be mounted on a mobile robot's body for further camera calibration. On the contrary, 3D calibration objects occupy more space and restrict movements of the robots, i.e. narrow down reachable workspace.

In this work a mobile robot with 4-DoF manipulator is employed. It is equipped with with four cameras installed on the robotic head. In order to be utilized in USAR related tasks, particularly, in visual inspection and 3D scene reconstruction of the destructed buildings or debris, cameras are required to be in calibrated state. Given estimated camera parameters – regardless of the chosen calibration approach – continuous changes in camera parameters during operation are inevitable. There might be multiple reasons for that, such as a varying weather conditions (for instance, changes in temperature and air pressure) and severe operation mode. Consequently, these factors lead to the accuracy and performance degradation. Thus, in order to mitigate a variation in visual sensor parameters a recalibration step is required.

In order to alleviate the camera parameters degradation issues we propose our solution which encompasses automatic camera calibration with on-board markers mounted on the mobile robot's body. One of the steps of 2D object-based calibration is a relative motions between a camera and a marker. For instance, in checkerboard calibration method the pattern should be viewed in at least 3 different positions relative to the camera. Therefore, it is necessary to estimate robotic arm joint configurations, i.e. find angles between the links of the manipulator, where camera can detect marker from various distances and angles. In our algorithm we solve for forward kinematics on a discretized set of joint angles. Subsequently, some of the estimated camera positions are manually checked so the camera can detect the marker. Conducted simulations and real pilot experiments demonstrated the algorithm's usability for further camera calibration.

The remainder of the paper is organized as follows. In Section 2 camera calibration approaches are reviewed. Then, a description of a Servosila Engineer's manipulator kinematics is provided in Section 3. Related work is further described in Section 4. Conducted experiments are provided in Section 5. Results from simulations and experiments on a real robot are outlined in Section 6. Finally, final conclusions are given and future plans are discussed at the end of this paper.

II. Camera Calibration

Camera calibration is the process of estimation of extrinsic and intrinsic parameters along with distortion coefficients. Intrinsic, or internal, parameters consists of internal camera's optical characteristics:

- principal point, i.e. 2D coordinates of the image plane center;
- focal length, i.e. distance between the camera lens and an image plane;
- skew coefficient;
- distortion coefficients of the lens.

The relation between the world and camera coordinate systems is determined by the extrinsic parameters. This relation is defined by a translation vector and a rotation matrix. Therefore, intrinsic and extrinsic parameters enable to transform objects from 3D space into an image plane – this is referred to as perspective projection.

2D pattern based camera calibration includes tracking of a planar pattern located at different poses relatively to the camera (Fig. 1) [16]. Compared to the 3D object based calibration

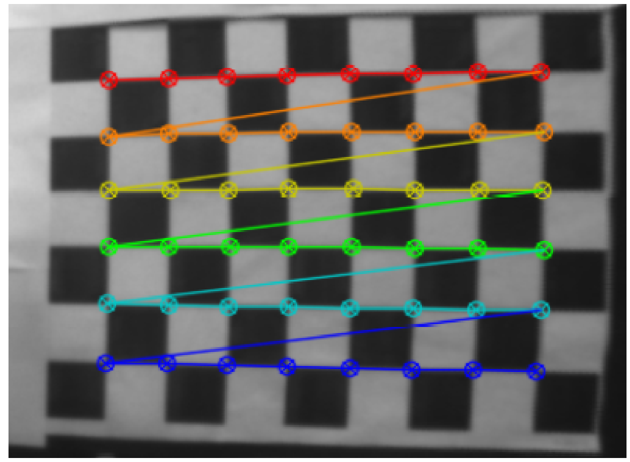

Fig. 1. Example of a planar pattern (8x6 checkerboard with white and black squares of equal size).

Fig. 2. Example of a 3D checkerboard pattern (two planes orthogonal to each other with checkerboard squares).

(Fig. 2), which makes use of up to three orthogonal planes, 2D object based calibration does not require complicated setup.

Generally, self-calibration approaches are less accurate compared to conventional methods [13] [17]. Reasons for inaccuracies of self-calibration methods are defined as follows:

- error in encoders as self-calibration methods exploit the known motion of a camera (mobile robot);
- influence of occlusions and lightning changes on feature detection and matching.

There are other advanced camera calibration techniques which try to enhance the accuracy of the camera parameters estimation in different environments. For example, spherical calibration objects can be used to lessen calibration pattern occlusion issues [18], whereas checkerboard pattern can be further modified to increase the accuracy of calibration in different light conditions using additional structural elements [9].

III. Robot Manipulator

In our work we used Servosila Engineer crawler-type mobile robot (Fig. 3) which is primarily designed for USAR [19]. It is equipped with four cameras located on the 4-DoF manipulator (Fig. 4): waist, shoulder, elbow, and neck. Joint variables (θ_i) limit values, i.e. the minimum and maximum angles between the links, are derived from both robot's technical reference and telemetry data (Table I).

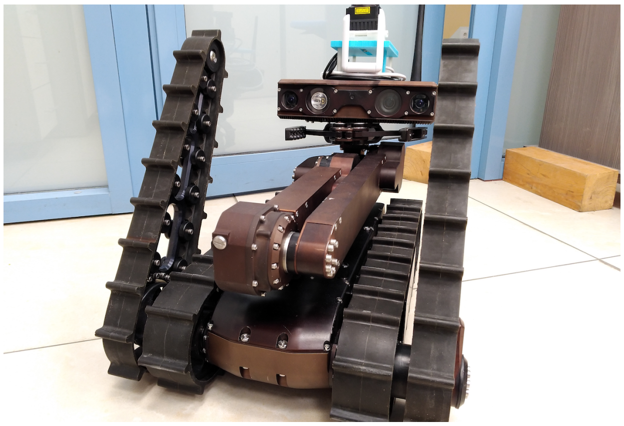

Fig. 3. Servosila Engineer crawler-type mobile robot (front view).

TABLE I
Reference and telemetry min-max values for joint variables of Servosila Engineer robot manipulator.

Joint	Min/max joint angles (degrees)	
	reference	telemetry
waist (θ_1)	-214.2 / 137.3	-213.88 / 136.09
shoulder (θ_2)	-16.4 / 114.2	2.47 / 114.2
elbow (θ_3)	-216.9 / 0	-216.9 / 0.06
neck (θ_4)	0 / 188.8	11.36 / 188.4

Fig. 4. Joints of the Servosila Engineer's manipulator.

TABLE II
D-H parameters describing kinematics of the Servosila Engineer's manipulator (each row describes a transformation from $(i-1)^{th}$ to i^{th} link).

i	r_i (mm)	α_i (rad)	d_i (mm)	θ_i (rad)
1	70	$\pi/2$	0	θ_1
2	300	0	0	θ_2
3	425	0	-60	$\theta_3 + \pi$
4	0	0	60	$\theta_4 - \pi$

Forward kinematics (FK) touches upon the problem of determining end-effector's position and orientation for the given joint variables (angles). Denavit-Hartenberg's (DH) notation can be used to describe a kinematic chain, i.e. four parameters describing the relationship between adjacent links of manipulator:

- r_i – link length, the distance from the Z_{i-1} to the Z_i axis along the X_i axis;
- α_i – twist, the angle between Z_{i-1} and Z_i axes around the X_i axis;
- d_i – offset, displacement from the X_{i-1} to the X_i axis along the Z_{i-1} axis;
- θ_i – the angle between X_{i-1} and X_i axes around the Z_{i-1} axis.

Model of Servosila Engineer's kinematic chain is demonstrated in Fig. 5. Each link is assigned with a coordinate frame, where Z_{i-1} is the axis of rotation of the i^{th} link. The transformation from the $(i-1)^{th}$ to the i^{th} link is described by the i^{th} row in Table II. It represents the following 4x4 homogeneous transformation matrix ($c \equiv \cos$ and $s \equiv \sin$):

$$
{}^{i}_{i-1}T = \left(\begin{array}{ccc|c} c\theta_i & -c\alpha_i \cdot s\theta_i & s\alpha_i \cdot s\theta_i & c\theta_i \cdot r_i \\ s\theta_i & c\alpha_i \cdot c\theta_i & -s\alpha_i \cdot c\theta_i & s\theta_i \cdot r_i \\ 0 & s\alpha_i & c\alpha_i & d_i \\ \hline 0 & 0 & 0 & 1 \end{array}\right) \tag{1}
$$

or

$$
{}^{i}_{i-1}T = \left(\begin{array}{c|c} {}^{i}_{i-1}R^3 & {}^{i}_{i-1}t \\ \hline 0^3 & 1 \end{array}\right),
$$

where ${}^{i}_{i-1}t$ – a translation vector from the $(i-1)^{th}$ to the i^{th} frame origin and ${}^{i}_{i-1}R^3$ – a 3x3 rotation matrix (orientation). Thus, given joint angles ($\theta_i, 1 \leq i \leq 4$), end-effector's position and orientation, i.e. forward kinematics, can be computed as the product of homogeneous transformations (from the 0^{th} to the 4^{th} frame):

$$
{}^{4}_{0}T = {}^{4}_{3}T \cdot {}^{3}_{2}T \cdot {}^{2}_{1}T \cdot {}^{1}_{0}T \tag{2}
$$

IV. Model building

A. Model in MATLAB

Obtained DH parameters are used to build a model of the robotic arm in MATLAB. Particularly, we make use of Robotics Toolbox for visualization purposes and to solve for

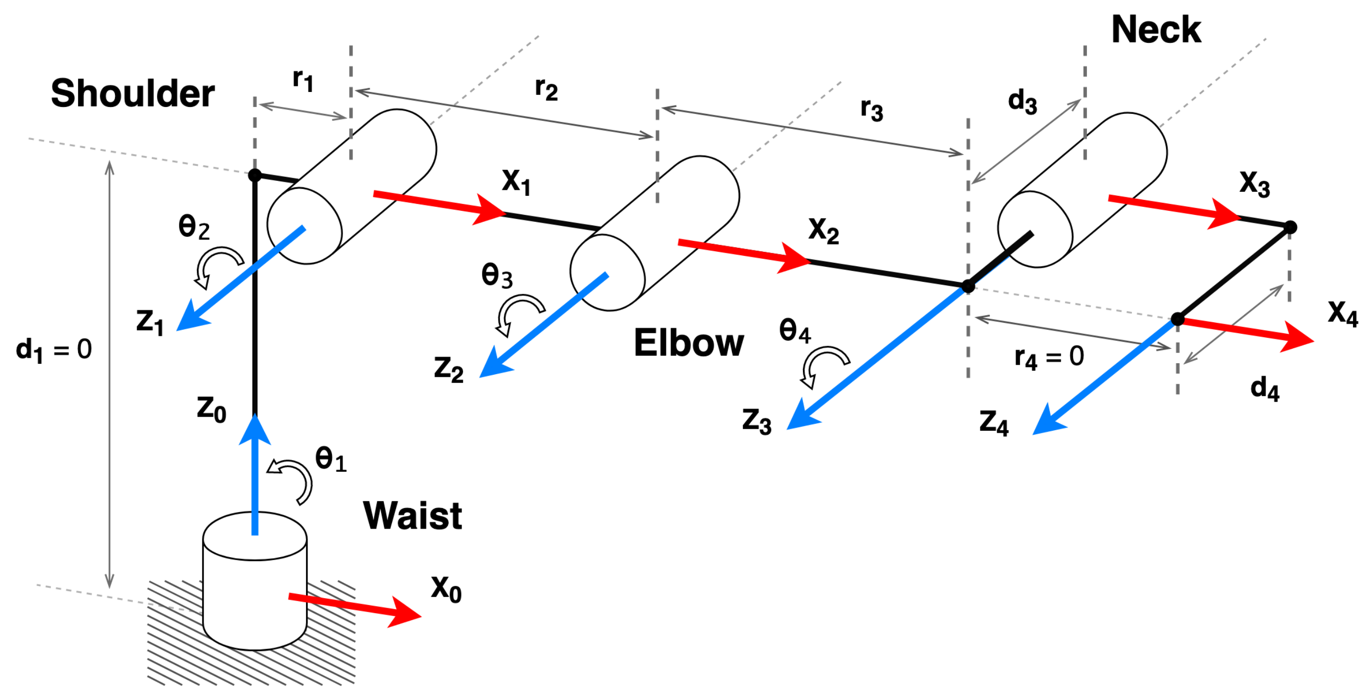

Fig. 5. Sketch of the Servosila Engineer's 4-DoF manipulator. Each link (black line) is attached with a (right-handed) coordinate system with the origin in the center of the revolute joint (cylinder). Z_i is the axis of rotation and θ_i is a positive direction of rotation for the i^{th} joint. Link length and offset are denoted as r_i and d_i, respectively. $(X_4 - Z_4)$ coordinate frame represents the end-effector of the manipulator (e.g. camera).

forward kinematics [20]. The model represents a set of links, consecutively connected by revolute joints. Length, offset, twist, and joint variable limits are specified for each link. Group of links forms the so-called serial link manipulator (Fig. 6). In this model we consider that the end-effector is a camera located on the robotic head. Camera viewing direction matches with the direction of the X-axis (Fig. 7).

Links are connected by revolute joints, whereas relations between links is defined by the derived DH parameters for the kinematic chain. The calibration pattern zone is designated with respect to the base frame, the origin of the manipulator's base (Fig. 7).

B. Joint configurations estimation

After analysis of possible marker positions on the mobile robot, considering possible marker size and ability of detecting it from different positions and orientations, it was decided to fix it on the robotic base above the battery section [21]. Proposed algorithm estimates positions and orientations of the robot manipulator's end-effector in which a marker with a high probability can be detected by the camera:

- Specify the position and dimension of the marker on the robotic base (Fig. 7, red zone).
- Exhaustive search – given reference joint angle limitations (Table I), go through the range of discretized joint angles (starting from the minimum angle up to the maximum one) and compute the position and orientation of the end-effector (camera), i.e. solve for FK for each joint configuration.

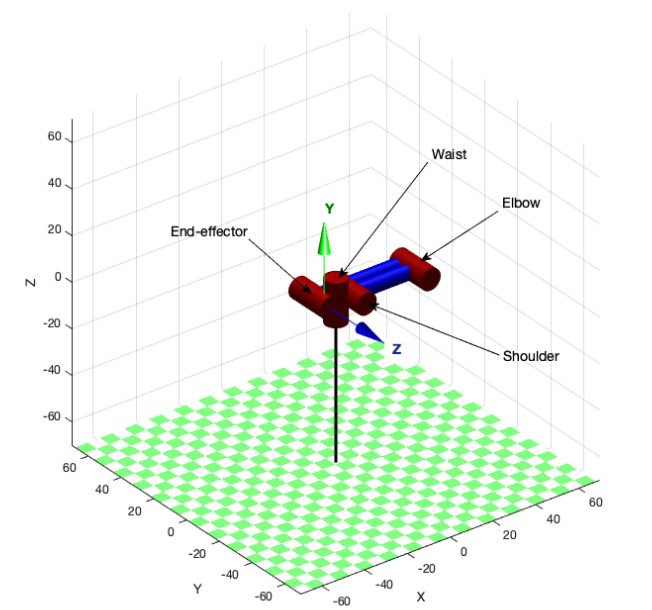

Fig. 6. Servosila Engineer robotic manipulator model in MATLAB. Joints and links are colored in red and blue, respectively. End-effector is assigned with a coordinate frame (green – Y-axis, blue – Z-axis). Base frame is denoted as a black vertical line.

- Given camera view direction, which is considered to be end-effector's X-axis (Fig. 7), determine its coordinates with respect to the manipulator's base frame.
- Compute the intersection point of the end-effector's X-

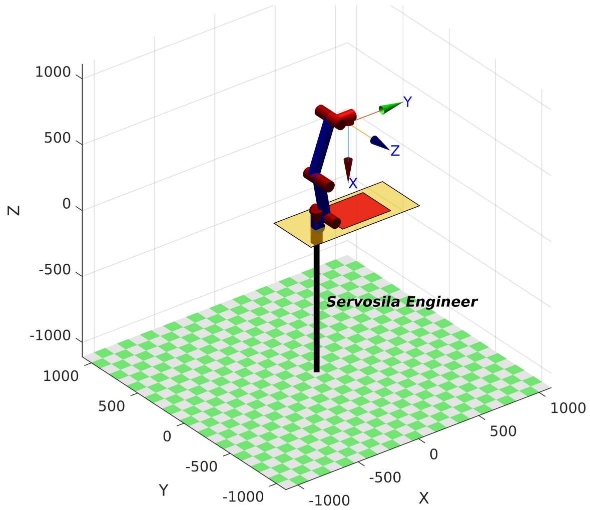

Fig. 7. Camera looking at the calibration pattern (in red).

axis and marker plane. We distinguish three cases depending on the location of the projection point: outside the marker zone, on the edge (vicinity) of the marker zone, and inside the marker zone. Points which are outside the zone are filtered out immediately, whereas points which are close the edges are kept for further analysis.

- Clustering. Total number of possible solutions is reduced up to a particular amount of configurations (approx. 100-200) by applying K-means clustering algorithm (Fig. 8).

V. Experiments

A. Simulations in MATLAB

During conducted experiments on estimation of camera calibration optimal joint configurations in MATLAB joint angles were discretized using 8, 10 and 20 degrees steps. As it is shown in Table III, with decreasing the discretization step number of solutions grow. For further analysis and to provide

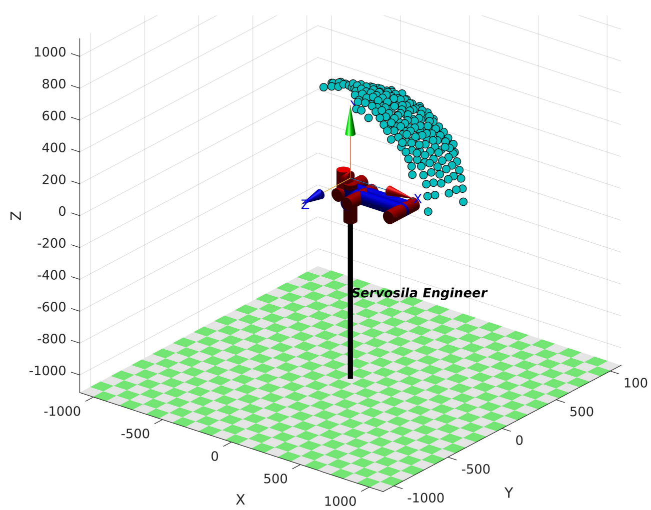

Fig. 8. A set of possible manipulator configurations after clustering.

TABLE III

Results of estimation of optimal joint configurations in MATLAB. Q – number of all joint configurations, Q' – number of optimal joint configurations (intersect with the marker plane).

Discretization step (deg)	Q	Q'
20	13860	365
10	210672	4525
8	502656	10735

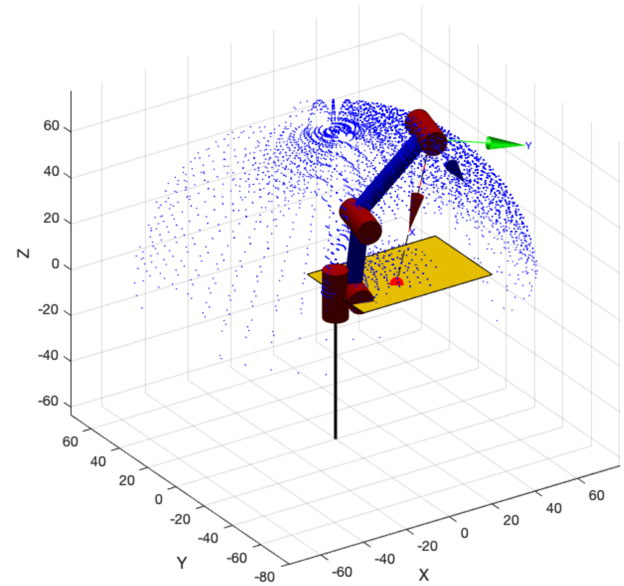

Fig. 9. Estimated camera locations (discretization step – 8 degrees, manipulator's joint configuration (in rad) – $[-0.24781.4591-0.644-2.618]$). Intersection point with the marker plane is denoted as a red dot.

data for experiments on a real robot estimated points are stored on a disk, which includes:

- the location of the camera, i.e. (x, y, z) coordinates and its orientation;
- coordinates of intersection point with the marker plane;
- joint configuration $[q1, q2, q3, q4]$.

It can be seen that all of the estimated camera locations for the given joint configurations are all inside a limited area - there are few camera positions close to the left and right sides of the base (Fig. 9).

B. Servosila Engineer

In order to verify obtained results, pilot experiments on a real robot were conducted. To verify if the Servosila Engineer can see its base, or the potential place for a calibration marker, the robot was manually controlled to reach the chosen state. To reach desired state pseudo-inverse kinematic was employed, i.e. using previously calculated relationships between the joint configuration and end-effector's position. Results vary depending on the ability of the robotic system to keep static stability and avoid self-collisions. In some cases the robot is statically

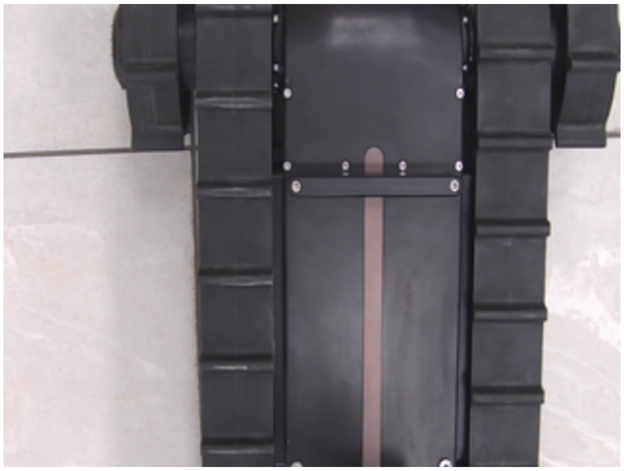

Fig. 10. Servosila Engineer in the statically stable position. View of the potential marker plane form the robot's on-board camera.

stable and can see the base (Fig. 10). Nevertheless, there are multiple states in which the ability to detect the marker is useless unless the robot is being helped to keep balance [22].

VI. Conclusions

In this work we developed an approach which helps to determine optimal joint configurations for the Servosila Engineer 4-DoF robot manipulator in order to automatically calibrate its camera. From the estimated positions the robot can detect the potential marker installed on its base, hence automatically calibrating its cameras by changing its joint configuration to the next one. The model of the robotic arm was built using which simulations were conducted in MATLAB environment. According to the obtained results, potential joint configurations for automatic camera calibration were discarded. Additionally, experiments on a real robot were conducted. Given simulation results some of the joint configurations were verified to be stable, whereas in other cases static stability and collision issues were faced. Therefore, as a part of our future work it is planned to improve the algorithms performance by using multi-threading techniques and to mitigate collision detection and static stability issues by modelling the robot in ROS/Gazebo.

Acknowledgment

The reported study was funded by the Russian Foundation for Basic Research (RFBR), project number 20-38-90257.

References

[1] E. Mingachev, R. Lavrenov, T. Tsoy, F. Matsuno, M. Svinin, J. Suthakorn, and E. Magid, "Comparison of ros-based monocular visual slam methods: Dso, ldso, orb-slam2 and dynaslam," in *International Conference on Interactive Collaborative Robotics*. Springer, 2020, pp. 222–233.

[2] C. Brand, M. J. Schuster, H. Hirschmüller, and M. Suppa, "Stereo-vision based obstacle mapping for indoor/outdoor slam," in *2014 IEEE/RSJ International Conference on Intelligent Robots and Systems*. IEEE, 2014, pp. 1846–1853.

[3] J. Salvi, X. Armangué, and J. Batlle, "A comparative review of camera calibrating methods with accuracy evaluation," *Pattern recognition*, vol. 35, no. 7, pp. 1617–1635, 2002.

[4] E. A. Martínez-García, J. Domínguez, and R. Lavrenov, "Dynamic modelling and control of an underactuated klann-based hexapod," in *2019 12th International Conference on Developments in eSystems Engineering (DeSE)*. IEEE, 2019, pp. 64–69.

[5] M. Fiala and C. Shu, "Fully automatic camera calibration using self-identifying calibration targets," *Techn. Rep*, vol. 48306, p. 26, 2005.

[6] J. Suriansky and M. Cmarada, "Analysis of methods for camera calibration in 3d scanning systems," *Annals & Proceedings of DAAAM International.–2012*, 2012.

[7] Z. Zhang, "Camera calibration," *Computer vision: a reference guide*, pp. 76–77, 2014.

[8] P. F. Sturm and S. J. Maybank, "On plane-based camera calibration: A general algorithm, singularities, applications," in *Proceedings. 1999 IEEE Computer Society Conference on Computer Vision and Pattern Recognition (Cat. No PR00149)*, vol. 1. IEEE, 1999, pp. 432–437.

[9] J. Liu, Z. Yang, H. Huo, and T. Fang, "Camera calibration method with checkerboard pattern under complicated illumination," *Journal of Electronic Imaging*, vol. 27, no. 4, p. 043038, 2018.

[10] O. D. Faugeras, Q.-T. Luong, and S. J. Maybank, "Camera self-calibration: Theory and experiments," in *European conference on computer vision*. Springer, 1992, pp. 321–334.

[11] G. Carrera, A. Angeli, and A. J. Davison, "Slam-based automatic extrinsic calibration of a multi-camera rig," in *2011 IEEE International Conference on Robotics and Automation*. IEEE, 2011, pp. 2652–2659.

[12] J. Kannala, J. Heikkilä, and S. S. Brandt, "Geometric camera calibration." *Wiley Encyclopedia of Computer Science and Engineering*, vol. 13, no. 6, pp. 1–20, 2008.

[13] F. Remondino and C. Fraser, "Digital camera calibration methods: considerations and comparisons," *International Archives of Photogrammetry, Remote Sensing and Spatial Information Sciences*, vol. 36, no. 5, pp. 266–272, 2006.

[14] B. Atcheson, F. Heide, and W. Heidrich, "Caltag: High precision fiducial markers for camera calibration." in *VMV*, vol. 10, 2010, pp. 41–48.

[15] A. Sagitov, K. Shabalina, L. Sabirova, H. Li, and E. Magid, "Artag, apriltag and caltag fiducial marker systems: Comparison in a presence of partial marker occlusion and rotation." in *ICINCO (2)*, 2017, pp. 182–191.

[16] H. Zollner and R. Sablatnig, *Comparison of methods for geometric camera calibration using planar calibration targets*. na, 2004.

[17] J. Kannala, J. Heikkilä, and S. S. Brandt, "Geometric camera calibration," *Wiley Encyclopedia of Computer Science and Engineering*, pp. 1–11, 2007.

[18] H. Zhang, K. W. Kwan-yee, and G. Zhang, "Camera calibration from images of spheres," *IEEE Transactions on Pattern Analysis and Machine Intelligence*, vol. 29, no. 3, pp. 499–502, 2007.

[19] I. Moskvin and R. Lavrenov, "Modeling tracks and controller for servosila engineer robot," in *Proceedings of 14th International Conference on Electromechanics and Robotics "Zavalishin's Readings"*. Springer, 2020, pp. 411–422.

[20] P. Corke, *Robotics, Vision and Control: Fundamental Algorithms In MATLAB® Second, Completely Revised*. Springer, 2017, vol. 118.

[21] T. Tsoy, A. Zakiev, K. Shabalina, R. Safin, E. Magid, and S. K. Saha, "Validation of fiducial marker systems performance with rescue robot servosila engineer onboard camera in laboratory environment," in *2019 12th International Conference on Developments in eSystems Engineering (DeSE)*. IEEE, 2019, pp. 495–499.

[22] E. Magid and T. Tsubouchi, "Static balance for rescue robot navigation: Discretizing rotational motion within random step environment," in *International Conference on Simulation, Modeling, and Programming for Autonomous Robots*. Springer, 2010, pp. 423–435.